The Journal of Foot & Ankle Surgery 60 (2021) 876−880

Contents lists available at ScienceDirect

The Journal of Foot & Ankle Surgery

journal homepage: www.jfas.org

Original Research

Load to Failure of the Ankle Joint Complex After Fusion of the Subtalar and Talonavicular Joints: A Cadaveric Study

Heidi M. Godoy, DPM, AACFAS[1], Michael Rotenberg, BS[2], Guido LaPorta, DPM, FACFAS[3], Ryan Willing, PhD[4]

[1] *Podiatric Resident Physician, PGY-III, Geisinger Community Medical Center, Scranton, PA*
[2] *MSME Student, Binghamton University, Binghamton, NY*
[3] *Director, Podiatric Medical Education, Geisinger Community Medical Center, Scranton, PA*
[4] *Assistant Professor, Mechanical Engineering Department, Binghamton University, Binghamton, NY*

A R T I C L E I N F O

Level of Clinical Evidence: 5

Keywords:
ankle joint complex
arthrodesis
coalition
cadaver
subtalar joint
talonavicular joint

A B S T R A C T

Recent literature has proposed that restriction of joints in the rearfoot secondary to coalitions may lead to increased risk for severe ankle fracture after trauma. There is a paucity of literature regarding the rigidity of the ankle joint after arthrodesis of the subtalar and talonavicular joints. In this study, load-to-failure testing of cadaveric ankle joints with and without fusion of the subtalar and talonavicular joints was performed to determine if clinically relevant fracture patterns could be reproduced. Of the 3 fixation patterns studied, combined subtalar and talonavicular joint fusion resulted in a measurable increase in joint stiffness; however, this was not statistically significant. Clinical and radiographic examination postloading revealed that all tested ankle joints sustained a dislocation type injury rather than a specific bone fracture pattern. It was determined that a pure low-speed bending and compression model does not produce clinically relevant fracture patterns, and that higher energy mechanisms are required.

The ankle joint complex has been described as a modified cardan joint and is made up of the talocrural joint (TCJ) and the subtalar joint (STJ). The axes of these joints are inclined to all 3 cardinal body planes. The obliquity of the ankle joint is such that it produces primarily sagittal plane motion. The obliquity of the STJ axis is such that it produces equal amounts of frontal and transverse plane motion, and to a much lesser degree, sagittal plane motion (1-4). Lundberg described the STJ as a “dampener” of motion between the foot and the leg, allowing dissipation of ground reactive forces as the body moves over the TCJ (5,6). Inman similarly refers to this phenomenon, calling the STJ a torque convertor (2). Several studies have commented on the restriction of adjacent joints when the STJ is fused (7-12) with Fortin reporting restriction of STJ motion up to 80% to 90% after an isolated fusion of the talonavicular joint (TNJ) (11).

With regards to other joints in the hindfoot, Astion found that simulated arthrodesis of the calcaneocuboid joint had little effect on the range of motion of the STJ, but reduced range of motion of the TNJ up to 67% (13). In addition, plantarflexion of the ankle after an isolated fusion of the TNJ has been shown to be decreased up to 10% (14).

The restriction of adjacent joints secondary to fusion of the STJ and TNJ continues to be a topic of interest in the literature. An understanding of rearfoot mechanics is critical for not only diagnosing pathology but treating rearfoot injuries. Recent literature has proposed that restriction of joints in the rearfoot secondary to coalitions, may result in less torsion being dissipated through the TCJ, resulting in severe fracture mechanisms after trauma (7,8). This could arguable raise similar concerns in rearfoot arthrodesis secondary to the similar restriction. This manuscript presents a study in which 3 of 6 cadaveric specimens' STJ and TNJs were fused and each ankle joint was loaded to failure. The purpose of this study was to test whether this experimental model could be used to elicit certain clinically relevant fracture patterns based on the arthrodesis performed.

Materials and Methods

Specimens

Three paired (6 total) fresh-frozen cadaveric limbs, transected at mid-tibia, were obtained from a limb bank. The small sample size was due to limited funds. Specimens are taken from 1 female and 2 male donors. The average age at the time of death was 65 years (range 57-79 years). Skin, subcutaneous tissue, and muscle were completely denuded from the most proximal portion of the limb; however, the interosseus ligament

Financial Disclosure: Funding for this study was provided by The American College of Foot & Ankle Surgeons Division 12 Tri State Region Educational Grant.

Conflict of Interest: None reported.

Address correspondence to: Heidi M. Godoy, DPM, AACFAS, Geisinger Community Medical Center, 15 Falcon PlWayne, NJ 07470

E-mail address: hgodoy15@gmail.com (H.M. Godoy).

1067-2516/$ - see front matter Published by Elsevier Inc. on behalf of the American College of Foot and Ankle Surgeons.
https://doi.org/10.1053/j.jfas.2020.09.009

Table 1
Description of rearfoot fixation patterns

	Right	Left
Specimen A	Control	STJ fused
Specimen B	Control	TNJ fused
Specimen C	Control	STJ + TNJ fused

of the ankle was kept intact. There was no macroscopic or radiographic evidence of injury, surgeries, osteoarthritis, or severe deformities. Varying amounts of STJ and TNJ arthrodesis were performed on left-sided limbs, while the contralateral limbs served as the control (Table 1). Fixation was achieved using 6.0 mm cannulated screws, and placement of screws was confirmed under fluoroscopy. Authors G.L. and H.G. performed the fixation techniques.

All specimens were prepared for biomechanical testing on a materials testing machine. This included denuding all soft tissues (including periosteum) from the tibia and fibula, starting approximately 6 cm proximal of the malleoli, leaving a clean bone surface for cement adhesion during potting. The tibia and fibula of each specimen were cemented inside individual segments of polyvinyl chloride (PVC)-piping using polymethyl methacrylate (Bosworth FastTray, Bosworth Company, Gibbstown, NJ). PVC segments were approximately 50 mm in diameter and 65 mm in length. Potting in PVC-pipe segments facilitated insertion and removal from a custom testing fixture connected to the vertical actuator of an MTS-858 Mini Bionix servohydraulic materials testing machine (Fig. 1, MTS, Eden Prairie, MN). Specimen containment bags loosely enclosed the entire foot and leg, sealing around the PVC pipe, to prevent leaking (Fig. 2).

The 6 specimens were individually placed onto the materials testing machine using 2 custom-designed testing fixtures (Fig. 3-4.) The hinged tray apparatus was used to convert the uniaxial compressive load into a combined compression and bending moment on each testing specimen, to reproduce an inversion-type motion of the ankle joint. As the compressive load was applied to the specimen, the tray would pivot and allow the ankle to invert. The specimens were loaded in uniaxial compression against the pivoting foot tray mounted to the static 5 kN load cell of the testing machine. This loading was chosen to simulate the weightbearing "rolling" or inversion of an ankle experienced during a typical ankle injury. Fig. 5 is a Computer Aided Design (CAD) model of the specimen on the MTS machine.

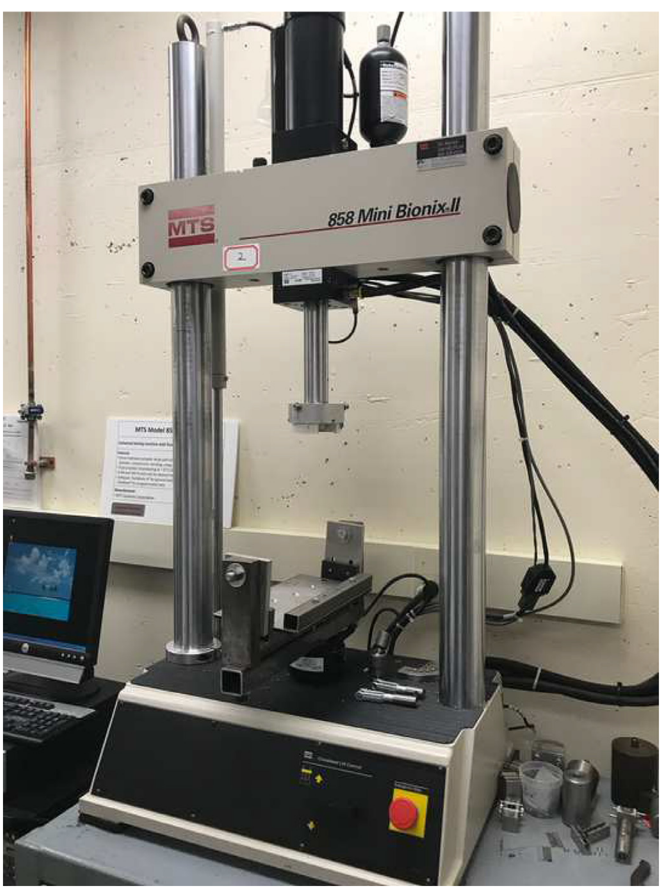

Fig. 1.

Fig. 2.

The specimens were tested on the MTS machine in force-control. An initial compressive load of 100 N was applied and held until the vertical compression of the foot on the plate reached equilibrium. This position was set as the zero-reference position for further compressive displacement. Each was then loaded in uniaxial compression with a constant loading rate of 500 N/min until failure. The data collected included force, displacement, and time. Data were sampled at a rate of 20 Hz. Failure was defined as either an audible cracking or visible failure of the ankle joint (ie, the foot displacing medially under the leg).

Specimens were clinically examined as well as radiographed postloading. Clinically, author H.G. inspected the tibia and fibula for any palpable fracture or signs of failure such as ligamentous laxity. Radiographically, anteroposterior and lateral foot and ankle x-rays were taken to evaluate for fracture.

Data Analysis

Collected data included the force versus displacement data for each specimen. For the purpose of comparing ankle joint strength, force versus displacement plots were analyzed, and the first peak in joint force was assumed to be the maximum failure load (loading beyond this point simply caused further joint damage). For the purpose of comparing ankle joint rigidity, the stiffness of each specimen was calculated based on the displacements measured at 50% and 90% of the respective

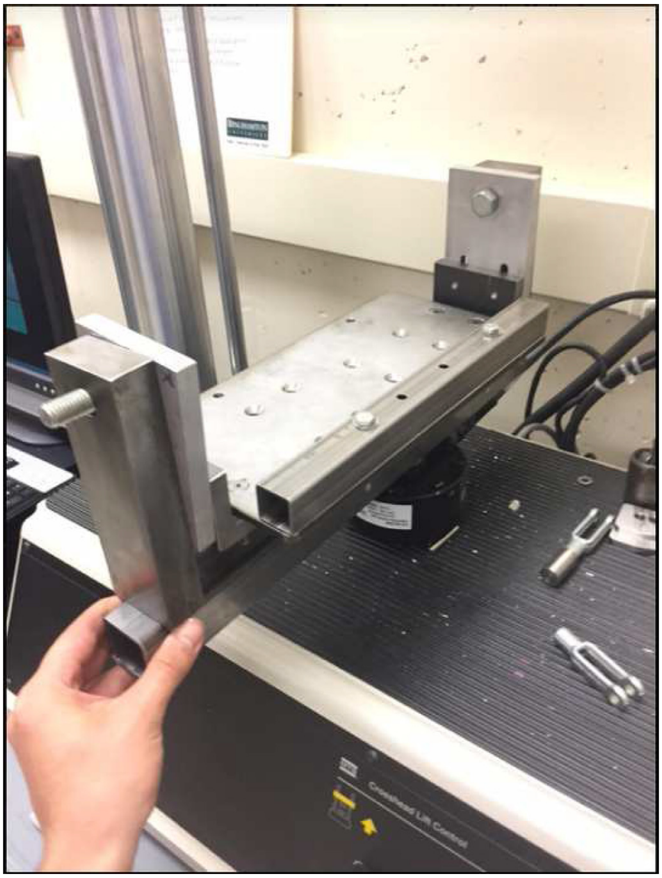

Fig. 3.

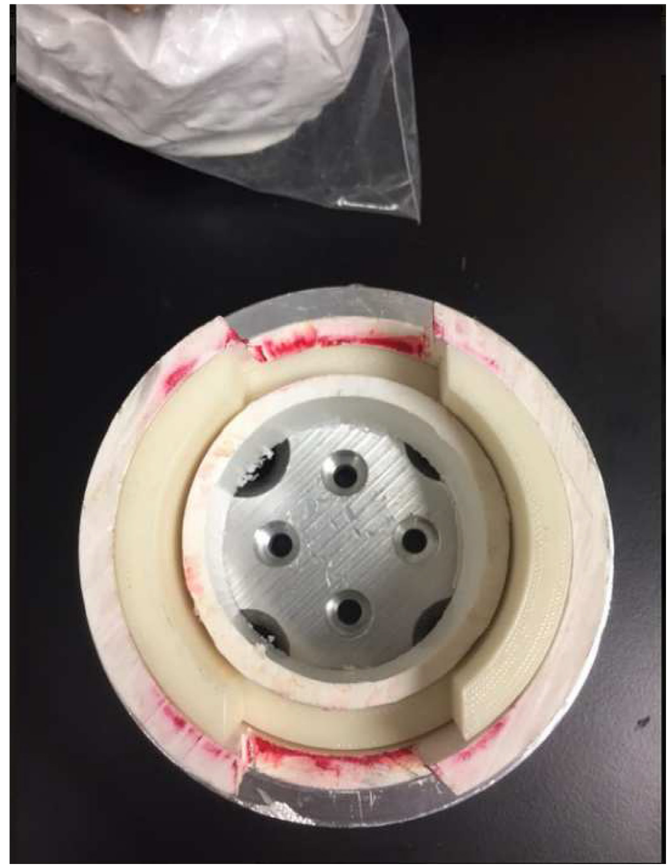

Fig. 4.

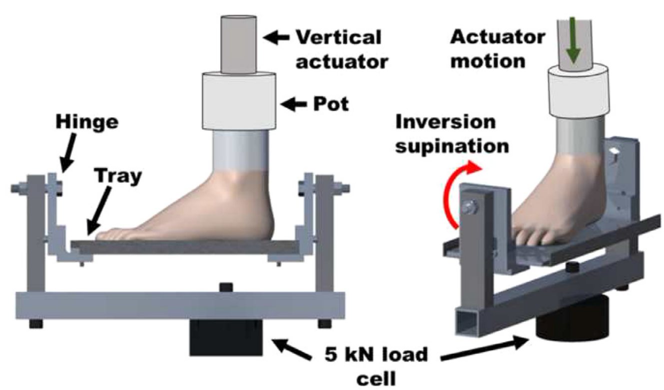

Fig. 5.

maximum failure loads. This span was selected based on visual approximation of the most linear portion of the force versus displacement curves of all 6 joints. Paired *t* tests were performed to detect possible differences in maximum force or stiffness due to joint fixation.

Results

Figures A, B, and C show the force versus displacement graphs of specimens A, B and C, respectively. The light gray lines represent the postfailure data that were omitted from any further analysis. The maximum force and stiffness data are summarized in Table 2. Considering all specimens, the fused joints were, on average, able to withstand higher maximum force than the unfused controls (2.0 ± 1.2 kN vs 1.4 ± 0.4 kN, respectively); however, the difference was not statistically significant (p = .3). The fused joints were also, on average, stiffer than the controls (146 ± 38 N/mm vs 99 ± 81 N/mm, respectively); however, the difference was not statistically significant (p = .3). In the first pair (Specimen A), the ST-fused joint initially seemed to have a lower stiffness than the control (unfused) joint; however, this joint eventually provided a stiffer response and failed at a higher load (Table 2). In the second pair (Specimen B), the control joint was stiffer and sustained a higher maximum force than the TN-fused joint throughout the entire load range. Specimen C, the joint which had both the ST and TN joints fused, was stiffer than the unfused control throughout the entire load range and sustained a higher maximum force.

Clinical exam postloading, in addition to radiographs taken post-study, revealed that the ankle joints sustained a dislocation type injury with no indication of fracture. No palpable defect was appreciated in the tibia or fibula and x-ray confirmed this (Fig. 4*a-c*).

Table 2
Maximum force and stiffness measured for each specimen

Specimen	Fixation	Maximum Force [kN]	Stiffness [N/mm]
A	ST joint fused	3.03	189
	Control	1.02	24
B	TN joint fused	0.68	117
	Control	1.82	184
C	ST + TN joints fused	2.16	131
	Control	1.24	88

Discussion

Common ankle fracture mechanisms include supination external rotation, pronation external rotation, pronation-abduction, and supination-adduction. Secondary to the type of machine used, we were only able to reproduce the supination-adduction type of injury The purpose of this study was to evaluate ankle fracture patterns along with stiffness after loading specimens with isolated fusions of the STJ and TNJ. In fact, none of the specimens tested in this study sustained the ankle fracture pattern which was anticipated. We postulate that the inability to fracture the ankle was due to several factors. First, the nature of the force used was a uniaxial compressive loading force with a constant loading rate, which differs from the typical high-energy impact type loading associated with acute ankle joint fractures. This was a limitation of the design of this study and the apparatus used. With this nonimpact loading scenario, the loaded specimens tended to fail due to TCJ dislocation rather than fracture of the lateral or medial malleolus. The dislocation occurred as the talus inverted under the tibia and the foot rolled under the leg. We attribute this not only to the type of loading force, but in addition, to the soft tissues surrounding the ankle joint complex. In acute ankle fracture injuries, viscoelastic behavior of the surrounding soft tissues would prevent sudden elongation and create larger joint reaction forces, resulting in fracture of the bones (15). In our cadaveric study, the soft tissues were able to slowly stretch as loading increased (no viscoelastic stiffening), reducing soft tissue tension and the overall joint reaction force. What followed was dislocation as the joint rolled excessively inward, preventing the fracture from occurring.

Second, complete soft tissue denuding proximally was necessary in order to cement the proximal tibia and fibula into the PVC pipe. The potential de-stabilizing role of this could have contributed to the atypical fracture mechanism that was appreciated. In hindsight, a syndesmotic screw could have been used to serve as stabilization.

Shin (16) studied the biomechanical and injury response of foot and ankles using finite element models under complex loading. They found that the talus and tibial plafond remain in contact during inversion/eversion loadings which stiffens the STJ. They also found that ligament failures were recorded at smaller tibial forces and large inversion angles. This is consistent with the results of our study when comparing larger inversion angles to soft tissue failure.

The fused Specimens A and C had a higher load to failure and stiffness compared to their controls; however, Specimen B did not. This could be secondary to the specific joint fused in Specimen B. Specimen B was the TN joint fusion, with no STJ fusion. Because Specimens A and C both had STJ fusions, this could mean that the STJ was the main contributor in locking up the TCJ. Also, we were looking to evaluate stiffness of the ankle joint and, for simplicity purposes, we did not measure the amount (although likely miniscule) of STJ motion in the control specimens. This could very well have played a role in the dampening effect /less stiff nature of Specimen B.

The maximum failure loads reported in this study were based on the first peak in the force versus displacement plots of each specimen. In some cases, the total force applied to the joint continued to increase, and secondary peaks were noted in the plots. Our rationale for selecting the first peak was that this would represent the first evidence of failure of anatomy. From our data, it was not possible to identify what the first failure mechanism within the joint was, because onset of total joint failure occurred very shortly after the initial peak and the specimens could not be inspected in between. This could be investigated further in future studies by employing a staged dissection approach, measuring the joint stiffness before and after incremental release of ankle joint stabilizers. Joint stiffness before failure was approximated as the slope of the force versus displacement plots from 50% to 90% of the maximum failure load. Some specimens exhibited large amounts of joint compression at relatively small loads; by using a lower cutoff of 50% of the maximum failure load, we intentionally omitted this portion of the data from stiffness calculations. Within this loading regime, we suspect that tissues were slowly being recruited and not fully tensioned until the more linear portion of the curve. This is akin to measuring the quasi-linear properties of tendons and ligaments while ignoring the toe and failure regions, which have been well described for many soft tissues (17).

There were several limitations to our study. First, we did not have fluoroscopy readily available during the experiment. This was secondary to the location of the loading apparatus and the inability to bring a machine into the department. We were confident in our clinical exam of the specimens after loading, however, could not be 100% certain without an x-ray.

A second limitation of our study was the small sample size and age groups represented. Brockett (3) commented on age and gender as influential factors that affect ankle joint range of motion and stiffness. They noted that with increasing age, females demonstrated less dorsiflexion and greater plantarflexion compared to male patients in the oldest age group. There was also a reduction in range of motion for both males and females in the oldest age groups. Having younger specimens may have changed our data, and more specimens or younger specimens may have given us the ability to change certain aspects of the design during the study, such as increasing the rate at which the specimens were loaded.

A third limitation was that a specific inversion angle for which the specimen was placed on the loading apparatus was not specified or measured. If we had used a standard angle of inversion for all of the specimens, we could have increased or decreased that angle to compare the effects on ankle stress.

If this experiment were to be repeated, the procedure would need to be altered to appropriately simulate the acute physiological fracturing mechanism that the ankle undergoes in trauma. The easiest way of doing this would be to use a testing machine able to provide an impulse load rather than a slower uniaxial load.

In conclusion, the authors found that a pure low-speed bending and compression model does not provide fracture patterns in the foot and ankle that can be studied and higher energy mechanisms are required. Despite the inability to fracture the ankles, this experimental procedure could be adapted for different applications relating to ankle inversion. The designed testing apparatus was able to successfully invert the ankle using an applied uniaxial compressive load. This design could serve as a reference for future experiments, specifically when specimens can only be loaded on one axis. Also, understanding the dampening role of soft tissues on the bone could provide authors with the importance of utilizing high force impacts should fracture be their primary goal. Overall, creating a cadaver model that approximates natural human physiological conditions is difficult. More research is needed to perfect the biomechanical foot and ankle model that approximates human physiology the best.

Declaration of Competing Interest

The authors declare that they have no known competing financial interests or personal relationships that could have appeared to influence the work reported in this paper.

References

1. Manter JT. Movements of the subtalar and transverse tarsal joints. Anat Rec 1941;80:397–410.
2. Stiehl JB. *Inmans's Joints of the Ankle*. Lippincott Williams &Wilkins, Philadelphia, 1991.
3. Brockett CL, Chapman GJ. Biomechanics of the ankle. Orthop Trauma 2016;30:232–238.
4. Siegler S, Udupa JK, Ringleb IS. Mechanics of the ankle and subtalar joints revealed through a 3D quasi-static stress MRI technique. J Biomech 2005;38:567–578.

5. Lundberg A, Goldie I, Kalin B, Selvik G. Kinematics of the ankle/foot complex:plantar flexion and dorsiflexion. Foot Ankle 1989;9:194–200.
6. Lundberg A, Svensson OK, Bylund C, Goldie I, Selvik G. Kinematics of the ankle/foot complex. Part 2: pronation and supination. Foot Ankle 1989;9:248–253.
7. Godoy HM, Micciche MJ. An incidental finding of a talonavicular and talocalcaneal joint coalition after a tibial pilon fracture: a case report. J Foot Ankle Surg 2017;56:1332–1334.
8. Imade S, Takao M, Nishi H, Uchio Y. Unusual malleolar fracture of the ankle with talocalcaneal coalition treated by arthroscopy-assisted reduction and percutaneous fixation. Arch Orthop Trauma Surg 2007;127:277–280.
9. Leardini A, Stagni R, O'Connor JJ. Mobility of the subtalar joint in the intact ankle complex. J Biomech 2001;34:805–809.
10. Hamel J, Müller G, Becker W. A case of bilateral isolated talonavicular synostosis in childhood−observations of tarsal joint function and functional adaptation of the proximal ankle joint. Z Orthop Ihre Grenzgeb 1993;131:275–277.
11. Fortin PT. Posterior tibial tendon insufficiency. Isolated fusion of the talonavicular joint. Foot Ankle Clin 2001;6:137–151.
12. Zhang K, Chen Y, Qiang M, Hao Y. Effects of five hindfoot arthrodeses on foot and ankle motion: measurements in cadaver specimens. Sci Rep 2016;6:354–393.
13. Astion DJ, Deland JT, Otis JC, Kenneally S. Motion of the hindfoot after simulated arthrodesis. J Bone Joint Surg Am 1997;79:241–246.
14. Mann RA, Beaman DN, Horton GA. Isolated subtalar arthrodesis. Foot Ankle Int 1998;19:511–519.
15. Pal S. *Mechanical properties of biologic materials. Design of Artificial Human Joints & Organs*. Springer, New York, 2014.
16. Shin J, Untaroiu CD. Biomechanical and injury response of human foot and ankle under complex loading. J Biomech Eng 2013;135:1–8.
17. Woo SL. Mechanical properties of tendons and ligaments. I. Quasi-static and nonlinear viscoelastic properties. Biorheology 1982;19:385–396.